Journal of the European Ceramic Society 20 (2000) 2759–2765

www.elsevier.com/locate/jeurceramsoc

The effect of sintering temperature variations on the development of electrically active interfaces in zinc oxide based varistors

C. Leach *, Z. Ling, R. Freer

Manchester Materials Science Centre, University of Manchester and UMIST, Grosvenor Street, Manchester M1 7HS, UK

Abstract

A series of zinc oxide based varistors containing 0.5 wt.% Bi_2O_3 and 0.5 wt.% Mn_2O_3 were prepared by a conventional mixed oxide route and sintered at temperatures between 950 and 1300°C. All samples showed the varistor effect, although as the sintering temperature was increased above 1000°C, the non-linear coefficient decreased from 22 to 3 at 1300°C. Local grain boundary property measurements were carried out using remote electron beam induced current (REBIC) configuration conductive mode scanning electron microscopy. The proportions of electrically active interfaces and those showing strong resistive contrast were found to increase with sintering temperature. © 2000 Elsevier Science Ltd. All rights reserved.

Keywords: Electrically active interfaces; Sintering temperature variations; Zinc oxide based varistors

1. Introduction

Zinc oxide varistors show highly non-ohmic current–voltage characteristics when subjected to high-voltage transients and are used with appropriate circuitry to shunt voltage spikes away from sensitive equipment. The non-ohmic properties are controlled by barrier structures developed at grain boundaries by the incorporation of segregating metal oxide additives. When present in sufficient quantity the segregating species form a distinct grain boundary film or layer.[1–3]

Grain boundary models for zinc oxide varistors can conveniently be divided into two main types; homojunction and heterojunction. The homojunction model[4] describes the varistor effect in terms of interactions between zinc oxide grains in close contact, with band bending occurring in the grain boundary region as a result of vacancy depletion during sintering, leading to an *n–i–n* structure. It has been suggested that in varistors the barrier height is increased by the introduction of specific metal oxide additives, such as bismuth, manganese and cobalt oxides.[4] The heterojunction model, on the other hand, assumes the presence of a discrete intergranular layer, comprising bismuth, cobalt, manganese and other oxides,[1] that provides acceptor states for electrons moving to the grain boundaries from within the *n*-type grains of zinc oxide. This results in a depletion region extending from either side of the grain boundary, giving rise to electronic band bending and an activation energy barrier to electron migration at the grain boundary interface. Both models predict that at low applied voltages electrons are prevented from crossing into adjacent grains and the material behaves in an insulating manner. At higher voltages electrons can tunnel into adjacent grains,[5] making the ceramic highly conducting. It has been demonstrated that individual grain boundaries with both thick (1 μm) and thin (< 500 Å) interfacial layers may show varistor behaviour.[6]

Sintering temperature is known to have a strong effect on varistor properties and frequently variations of a few 10's of degrees in the maximum temperature attained can give rise to noticeable differences in varistor performance.[7] These changes are generally quantified in terms of bulk performance parameters such as the non-linear coefficient, α or leakage current, rather than by observing local variations in behaviour due to differences in interfacial structure or composition. There is increasing evidence that in a typical varistor, differences occur in the current–voltage response of individual grain boundaries[8] and that some grain boundaries do not show a varistor effect at all.[9] In order to study the consequences of these differences it is therefore essential that the characterisation techniques used include those

* Corresponding author. Tel.: +44-161-200-3561; fax: +44-161-200-3586.

E-mail address: colin.leach@man.ac.uk (C. Leach).

PII: S0955-2219(00)00223-5

that investigate the properties of the material on the scale of the individual grain boundary, as well as bulk measurements, enabling direct correlation between grain boundary structures and bulk properties to be made.

Remote electron beam induced current (REBIC) microscopy is a SEM based technique that is a form of the conductive mode of operation,[10,11] providing localised information about the structure of individual electrically active and inactive interfaces in electrical ceramics and any conduction mechanisms that may occur locally. The technique has been used to characterise many semi-conducting materials and wide bandgap semiconductors, including zinc oxide.[10–18] The current providing the image-forming signal is collected from two electrodes placed on the sample surface on either side of the area of interest (Fig. 1). Variations in the current flowing to earth through each electrode, or currents generated by the separation of beam induced electron-hole pairs at built-in fields within the sample result in contrast variations that maybe observed, with a spatial resolution of the order of the excitation volume.

In zinc oxide based varistors three distinct types of REBIC signal have been observed, coincident with individual grain boundaries. These occur either singly, or in combination, and are classified according to their image contrast as:

Type I	consisting of adjacent, parallel dark and bright lines;
Type II	consisting of single dark or bright line; and
Type III	consisting of a step change in brightness.

Complementary contrast effects are not observed in secondary or backscattered electron images of the same area and therefore the conductive mode contrast cannot be due to the modulation of the absorbed beam current by emitted electrons.

Types I and II contrast are formed by the collection of currents generated by the separation of beam induced electron-hole pairs in the depletion regions of charged grain boundaries. If the grain boundary is symmetrical, the opposed electric fields on either side of the grain boundary give rise to EBIC currents of opposite sign, resulting in type I contrast, comprising adjacent bright/dark lines parallel to the grain boundary in EBIC images (Fig. 2). If the grain boundary is asymmetrical and the EBIC signal from one side of the grain boundary is inhibited, then type II contrast is seen. Grain boundaries where types I and II contrast effects occur are considered to be electrically active.

Type III contrast arises because the specimen acts as a current divider, channelling the absorbed current between the two current collecting electrodes placed on either side of the region of interest.[11] In an homogeneous sample there is a linear variation in the proportion of signal passing through each electrode as the primary beam scans the inter-electrode region. Local heterogeneities in sample resistivity result in changes to this gradient and are observed in images as steps in the brightness level. When this occurs at a resistive grain boundary, it gives rise to type III contrast. In situations where no type I or type II contrast is observed, the barrier is considered to be electrically inactive.

In this contribution we compare the microstructural and local electrical property development

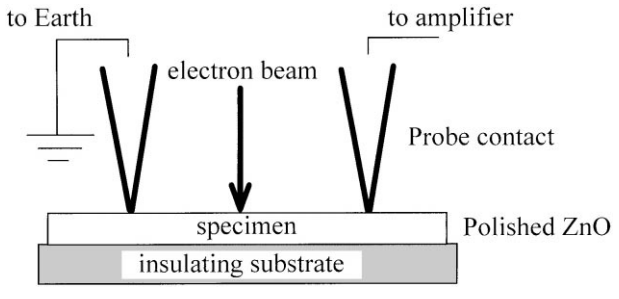

Fig. 1. The sample configuration used for conductive mode imaging.

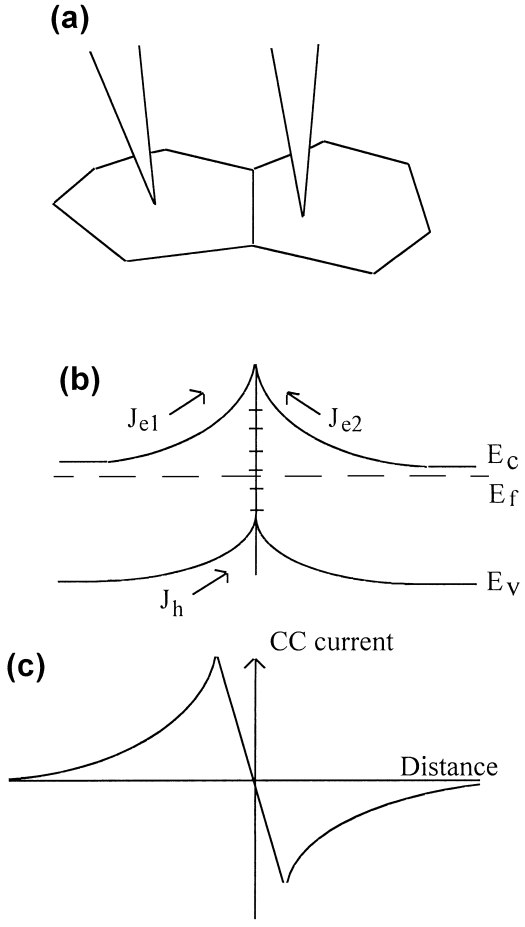

Fig. 2. Sample configuration (a), energy band diagrams (b), and the corresponding charge collection contrast profile (c) for a varistor grain boundary where charge separation effects occur (from Ref. 18).

of an isochemical series of varistors sintered at temperatures between 950 and 1300°C.

2. Experimental method

A simplified varistor composition based on zinc oxide doped with 0.5 wt.% Bi_2O_3 and 0.5 wt.% Mn_2O_3 was prepared by a standard mixed oxide route. Standard 10 mm diameter and 2 mm thick compacts were formed by uniaxial pressing at 170 MPa and sintered at temperatures between 950 and 1300°C for 2 h in air using heating and cooling rates of 100°C/h. Polished surfaces were prepared for SEM analysis by grinding a flat face on SiC paper, polishing with progressively finer grades of diamond paste and finally lapping with a water based slurry of 0.3 μm α-alumina powder. The samples were mounted on insulating stubs and observed in Philips 525 and XL7 SEM's using the secondary electron, backscattered and conductive modes of operation. For the conductive mode imaging, two electrodes, whose positions were controlled by a micromanipulator, were placed directly in contact with the material on either side of the region of interest, forming ohmic electrical contacts and enabling collection of the signal for amplification with a commercial EBIC amplifier.

After REBIC analysis, the samples were lightly etched using a 2% acetic acid solution for 2 min in order to delineate all grain boundaries and permit grain size measurements to be made using the ASTM intercept method.[19]

Current–voltage measurements were carried out on the bulk samples using an adjustable DC power supply (Brandenberg 475R) operating in the range 10–1700 V. The non linear exponent (α) was determined for each sample from I–V plots using current densities of 0.1 and 1 $mAcm^{-2}$ according to the equation;

$$\alpha = \log(J_2/J_1)/\log(E_2/E_1) \quad (1)$$

where E_1 and E_2 represent the electrical fields across the sample at current densities J_1 and J_2.

3. Results

Fig. 3 shows a series of backscattered electron images of the varistors sintered at temperatures between 950 and 1300°C, to densities between 90 and 95% of theoretical. In these images the zinc oxide grains are differentiated through differences in channelling contrast. A bismuth rich phase is clearly visible as bright patches at grain boundaries and, particularly, at triple points within the microstructure of the 950°C sintered sample (Fig. 3a). In the 1000°C sintered sample (Fig. 3b) the bismuth rich phase appears to have wetted the majority of the grain boundaries, although isolated pockets remain at triple points and close to pores. Some grain growth has occurred in this sample, giving rise to a few large grains in a finer groundmass. At sintering temperatures of 1100°C and above (Fig. 3c–e), significant grain growth has occurred leaving residual 5–10 μm diameter pores both at grain boundaries and within some grains. The bismuth rich grain boundary film is not generally detectable in these samples except as small isolated pockets. The grain sizes of these samples were measured from secondary electron images of polished and etched samples, and are presented in Table 1.

Fig. 4 shows a series of partial I–V characteristics of the sintered varistors from which the values of the non-linear coefficient, α, were calculated (Table 1). α Reaches a peak value of 22 for a sintering temperature of 1000°C, after which there is a progressive reduction with the 1300°C sample showing only a weak varistor effect.

REBIC images of the sample series are presented in Fig. 5. Two distinct types of REBIC signal occur within these samples: charge collection currents giving rise to type I and type II contrast effects at electrically active grain boundaries, and step changes of brightness giving rise to type III contrast effects at resistive grain boundaries.

In the 950 and 1000°C sintered samples (Fig. 5a and b), charge collection contrast is seen as disjointed bright or dark lines, coincident with some grain boundaries. The contrast is predominantly type II, comprising single bright or dark lines, although there is also some type I contrast present. There is also a smooth background resistive contrast gradient, from dark on the left to bright on the right, running across the sample. Brightness steps are seen occasionally at some grain boundaries, where the local resistivity is high.

In the samples sintered at temperatures of 1100°C and above (Fig. 5c–e), grain growth has resulted in a coarser microstructure. Type I charge collection contrast is visible throughout the samples; with some grain boundaries showing type II contrast. The electrically active grain boundaries frequently form connected arrays through the sample. Resistive contrast is clearly visible as brightness steps coincident with some grain boundaries, giving rise to a terraced microstructure. In general, the terrace boundaries coincide with electrically active interfaces although not all of each terrace boundary is electrically active.

Table 1 lists the percentage of electrically active interfaces in each sample. As previously indicated electrical activity in this context is defined by the interface showing type I or type II EBIC contrast, rather than implying varistor characteristics. The proportion of electrically active grain boundaries increases steadily with increasing sintering temperature, although even in the 1300°C sintered sample fewer than 50% of all grain boundaries show electrical activity. Equal proportions of bright and dark type II contrast occur within each sample.

4. Discussion

As the sintering temperature is increased above 1000°C, the percentage of electrically active grain boundaries increases, although α decreases. In these samples there does not appear to be a direct link between the non-linear coefficient and the proportion, or density, of electrically active grain boundaries. The progressive reduction in α, after reaching a peak value of 22 for a sintering temperature of 1000°C, is attributed

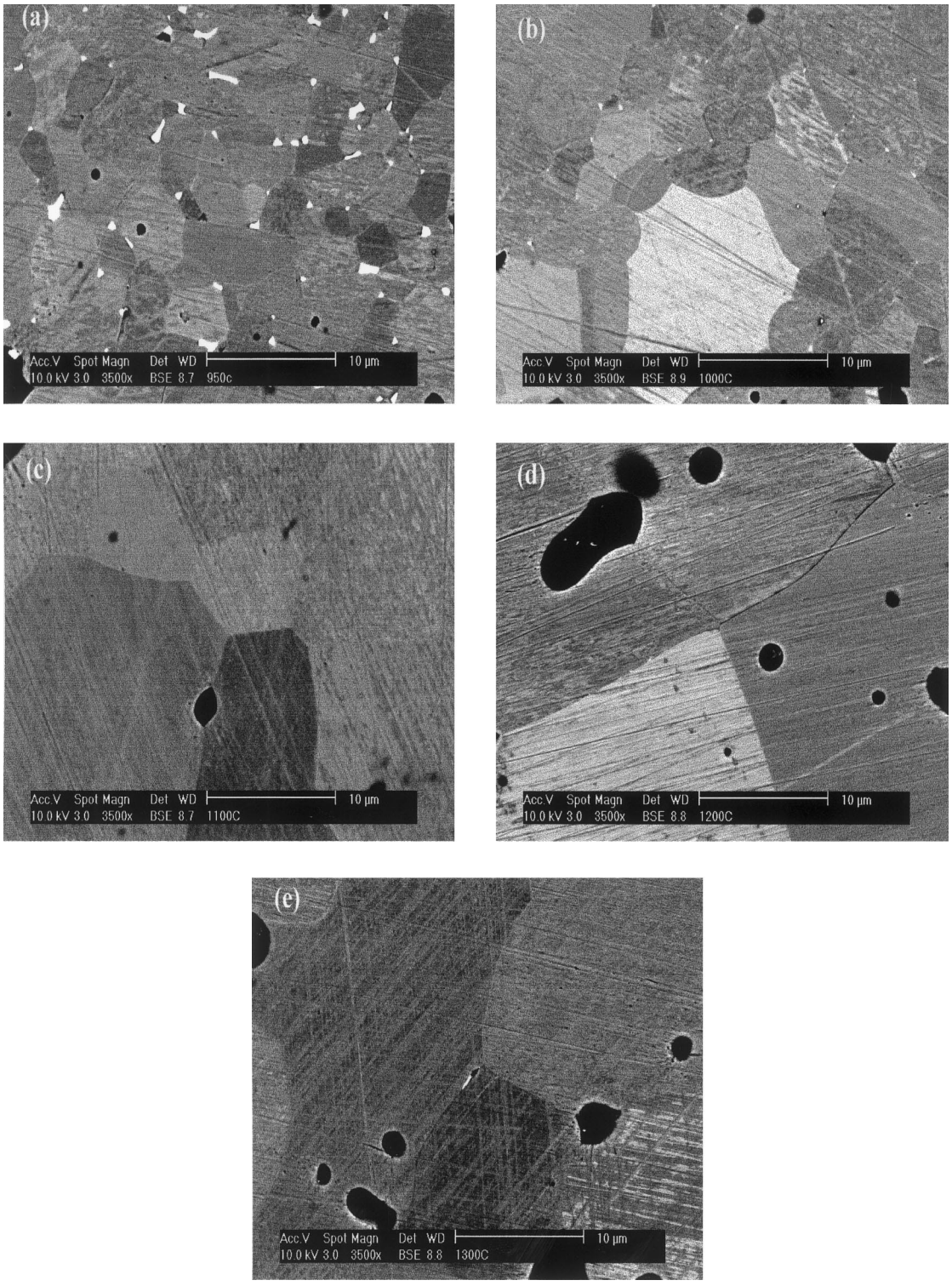

Fig. 3. Backscattered electron images showing the effect of variations in sintering temperature on the distribution of Bi-rich phases present in the samples sintered at (a) 950°C; (b) 1000°C; (c) 1100°C; (d) 1200°C; (e) 1300°C. Scale bar = 10 µm.

Table 1
The variation of grain size, α and the percentage of electrically active interfaces with sintering temperature

	Sintering temperature				
	950°C	1000°C	1100°C	1200°C	1300°C
Mean grain size (μm)	6	8	15	39	49
α	19	22	12	10	3
Percentage of electrically active grain boundaries	–	14	26	32	47

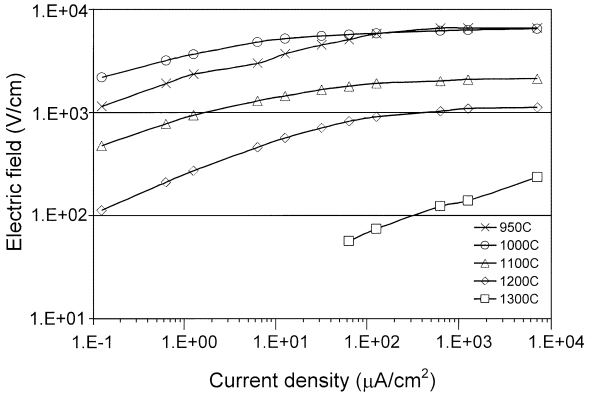

Fig. 4. Partial *I–V* characteristics, plotted as electric field strength vs. current density, for the varistors prepared in this study.

to a lowering of the grain boundary barrier height with increased sintering temperature.[20] The presence or absence of EBIC contrast is not directly related to the grain boundary barrier height, although for EBIC contrast to be present there must be built-in fields within the sample caused by band bending at a charged grain boundary. Any change in proportion of electrically active grain boundaries must therefore be related to some other aspect of the interfacial structure.

In a related study, local transitions between type I (electrically active) and type III (electrically inactive) grain boundary contrast were observed along the length of a single varistor grain boundary.[18] The grain boundary contained a bismuth rich film of variable thickness that was clearly visible in the secondary electron image. Type III contrast was observed coincident where the film was thickest and type I contrast occurred where the film thinned. Thus electrically active grain boundaries appear to be associated with thin grain boundary films.

In another study, the extent of grain boundary wetting in varistors doped with Bi_2O_3 and CoO was found to increase from 0% at the $ZnO–Bi_2O_3$ eutectic temperature to 88% at 1140°C while the average dihedral angle of the films at the grain junctions decreased monotonically with increasing sintering temperature.[21] Further, a reduction in the total volume of bismuth rich phase due to volatilisation as the sintering temperature increased was shown to cause it to congregate at the triple junctions, leaving only a partial coverage along the grain boundaries.[22] In the samples studied here, all show the varistor effect, indicating that a bismuth rich phase has segregated to grain boundaries in all of the samples. Thus, since EBIC contrast is particularly sensitive to the presence of built-in fields at charged grain boundaries, its detection at an increasing proportion of grain boundaries as the sintering temperature is increased reflects a more extensive coverage of a thin film of bismuth rich phase, and its retention along the grain boundaries, as the total volume decreases, is believed to be due to volatilisation at the higher sintering temperatures.

In the samples studied here, electrically active grain boundaries showing type II contrast are much more common than those showing type I contrast. This observation concurs with previous studies[23,24] but is difficult to explain since the EBIC contrast expected from a symmetrical charged grain boundary is type I (Fig. 2). The more common type II contrast occurs when only one side of the interface shows electrical activity, giving rise to a single contrast line. By applying a small, external voltage bias, of the order of 10's of mV, across a grain boundary showing type II contrast, electrical activity can be restored in the inactive side of the interface, causing the grain boundary to show type I contrast. Likewise a grain boundary showing type I contrast can be modified to show either bright or dark type II contrast by applying a small bias voltage.[25] This occurs because the electric field associated with the externally applied bias progressively compensates the electric field on one side of the grain boundary, giving rise to flat band conditions. On the side where the bands are flattened, no charge separation can occur and hence no EBIC signal is observed. The side of the interface where the flat band conditions are induced depends on the polarity of the applied potential across the grain boundary, and hence the direction of the applied electric field. Changing the sign of the voltage bias applied to an interface originally showing type I contrast will cause the resultant type II contrast to switch from dark to bright.

Strong type III contrast is indicative of high resistivity grain boundaries that have previously been attributed to relict agglomerate surfaces from the pre-sintered powder structure[17]; the high interfacial resistivity being caused by the effects of a surface build up of dopants, particularly manganese, on the agglomerated powder, during powder preparation. The increase in sample resistivity with manganese doping concurs with the findings of Einzinger[4] who noted that polycrystalline zinc oxide doped with 1% MnO was highly resistive, compared with the undoped material. In this study, the strong type III contrast observed in samples sintered at

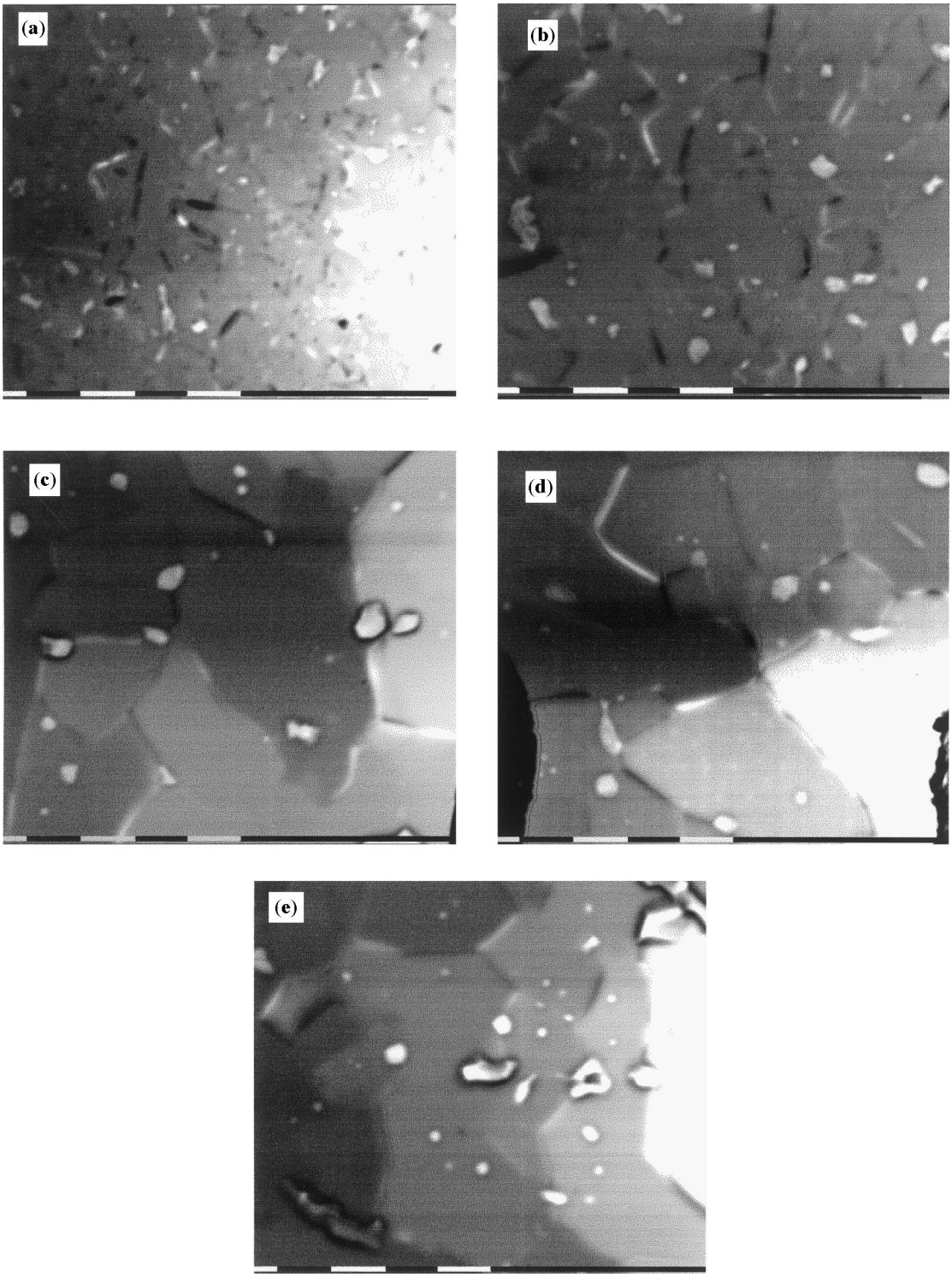

Fig. 5. REBIC images showing the effect of variations in sintering temperature on the distribution of electrically active interfaces. Samples were sintered at (a) 950°C; (b) 1000°C; (c) 1100°C; (d) 1200°C; (e) 1300°C. Scale bar = 10 μm.

1100°C and above indicates that, as grain growth occurs, this resistance increase is predominantly localised to the grain boundaries. The superimposed EBIC signals indicate that many of the interfaces have developed a highly resistive grain boundary structure, which is also electrically active.

5. Conclusions

A series of zinc oxide based varistors containing 0.5 wt.% Bi_2O_3 and 0.5 wt.% Mn_2O_3 were prepared by a conventional mixed oxide route and sintered at temperatures between 950 and 1300°C. It was found that:

1. Grain growth became significant in samples sintered at temperatures in excess of 1000°C.
2. All samples showed the varistor effect, and the peak value of the non-linear coefficient, α, was found to be 22, occurring at a sintering temperature of 1000°C.
3. The percentage of electrically active grain boundaries increased steadily with increasing sintering temperature.
4. In the samples sintered at 1100°C and above, many electrically active interfaces also showed strong resistive contrast.

References

1. Matsuoka, M., Non-ohmic properties of zinc oxide ceramics. *Jpn. J. Appl. Phys.*, 1971, **10**, 736–746.
2. Levinson, L. M. and Phillip, H. R., The physics of metal oxide varistors. *J. Appl. Phys.*, 1975, **46**, 1332–1341.
3. Eda, K., Conduction mechanism of non-ohmic zinc oxide ceramics. *J. Appl. Phys.*, 1978, **49**, 2964–2972.
4. Einzinger, R., Metal oxide varistor action — a homojunction breakdown mechanism. *Appl. Surf. Sci.*, 1978, **1**, 329–340.
5. Mahan, G.D,. Levinson M. and Phillip, H. R., Theory of conduction in ZnO varistors. *J. Appl. Phys.*, 1979, **50**, 2799–2812.
6. Olsson, E., Dunlop, G. and Osterlund, R., Characterisation of individual interfacial barriers in a ZnO varistor material. *J. Appl. Phys.*, 1989, **66**, 3666–3675.
7. Asokan, T. and Freer, R., Dependence of ZnO varistor grain-boundary resistance on sintering temperature. *J. Mater. Sci. (Lett.)*, 1994, **13**, 925–926.
8. Tao, M., Ai, B., Dorlanne, O. and Loubiere, A., Different single grain junctions within a ZnO varistor. *J. Appl. Phys.*, 1987, **61**, 1562–1567.
9. Hohenberger, G. and Tomandl, G., Inhomogeneous conductivity in varistor ceramics: methods of investigation. *J. Am. Ceram. Soc.*, 1991, **74**, 2067–2072.
10. Bubalek, L. O. and Tennent, W. E., Observation of charge separating defects in HgCdTe using remote contact electron beam induced current. *Appl. Phys. Lett.*, 1988, **52**, 1255–1257.
11. Russell, J. D. and Leach, C., Problems associated with imaging resistive barriers in PTC thermistor ceramics using the SEM conductive mode. *J. Eur. Ceram. Soc.*, 1995, **15**, 617–622.
12. Mataré, H. F. and Laaksoo, C. W., Space-charge domains at dislocation sites. *J. Appl. Phys.*, 1969, **40**, 476–482.
13. Panin, G. N. and Yakimov, E. B., *Temperature dependent EBIC contrast investigations of grain boundaries and precipitates in CdTe*. Institute of Physics Conference, Series No. 117, Bristol, 1991, pp. 763–766
14. Holt, D. B., Local grain boundary property measurements. *Sol. State Phenom.*, 1994, **37**(38), 171–182.
15. Bernds, A., Loehnert, K. and Kubalek, E., SEM EBIC investigations of ZnO varistor ceramics. *J. Phys. Coll.*, 1984, **C2**, 861–864.
16. Van Kemenade, J. T. C. and Eijenthoven, R. K., Direct determination of barrier voltage in ZnO varistors. *J. Appl. Phys.*, 1979, **50**, 938–941.
17. Halls, D. C. and Leach, C., Processing induced resistive barriers in ZnO varistor material. *J. Mater. Sci.*, 1995, **30**, 2733–2737.
18. Russell, J. D., Halls, D. C. and Leach, C., Direct observation of grain boundary Schottky barrier behaviour in zinc oxide varistor material. *J. Mater. Sci. (Lett.)*, 1995, **14**, 676–678.
19. Van der Voort, G. F., Grain size measurement. In *Practical Applications of Quantitative Metallography. ASTM STP 839*, ed. J. L. McCall and J. H. Steele. American Society for Testing and Materials, Philadelphia PA, 1984, pp. 85–131.
20. Shim, Y. and Cordaro, J. F., Admittance spectroscopy of polycrystalline ZnO–Bi_2O_3 and ZnO–BaO systems. *J. Am. Ceram. Soc.*, 1988, **71**, 184–188.
21. Gambino, J. P., Kingery, W. D., Pike, G. E., Levinson, L. M. and Philipp, H. R., Effect of heat-treatments on the wetting behaviour of bismuth- rich intergranular phases in ZnO-Bi-Co varistors. *J. Am. Ceram. Soc.*, 1989, **72**, 642–645.
22. Lee, J. R. and Chiang, Y. M., Bi segregation at ZnO grain boundaries in equilibrium with Bi_2O_3-ZnO liquid. *Sol. State Ionics*, 1995, **75**, 79–88.
23. Russell, J. D., Halls, D. C. and Leach, C., Grain boundary SEM conductive mode contrast effects in additive free ZnO ceramics. *Acta Mater. Metallur.*, 1996, **44**, 2431–2436.
24. Russell, J. D., Halls D. C. and Leach, C., The relationship between crystal misorientation and conductive mode contrast of grain boundaries in additive free zinc oxide. *J. Mater. Sci.*, 1997, **32**, 4585–4589.
25. Leach, C., *Interface Science*, 2000, in press.